Electronic Supplementary Information (ESI)

Boron nitride nanosheets with controlled size and thickness for enhancing mechanical properties and atomic oxygen erosion resistance

Lei Liu,[ac] Zhigang Shen,*[ab] Yiting Zheng,[c] Min Yi,[ab] Xiaojing Zhang[a] and Shulin Ma[a]

[a] Beijing Key Laboratory for Powder Technology Research and Development, Beijing University of Aeronautics and Astronautics, Beijing 100191, China.

[b]Ministry of Education Key Laboratory of Fluid Mechanics, Beijing University of Aeronautics and Astronautics, Beijing 100191, China

[c] School of Material Science and Engineering, Beijing University of Aeronautics and Astronautics, Beijing 100191, China

E-mail: *shenzhg@buaa.edu.cn*

Table of contents:

TC1: effects of BNNSs on reducing bubble defects

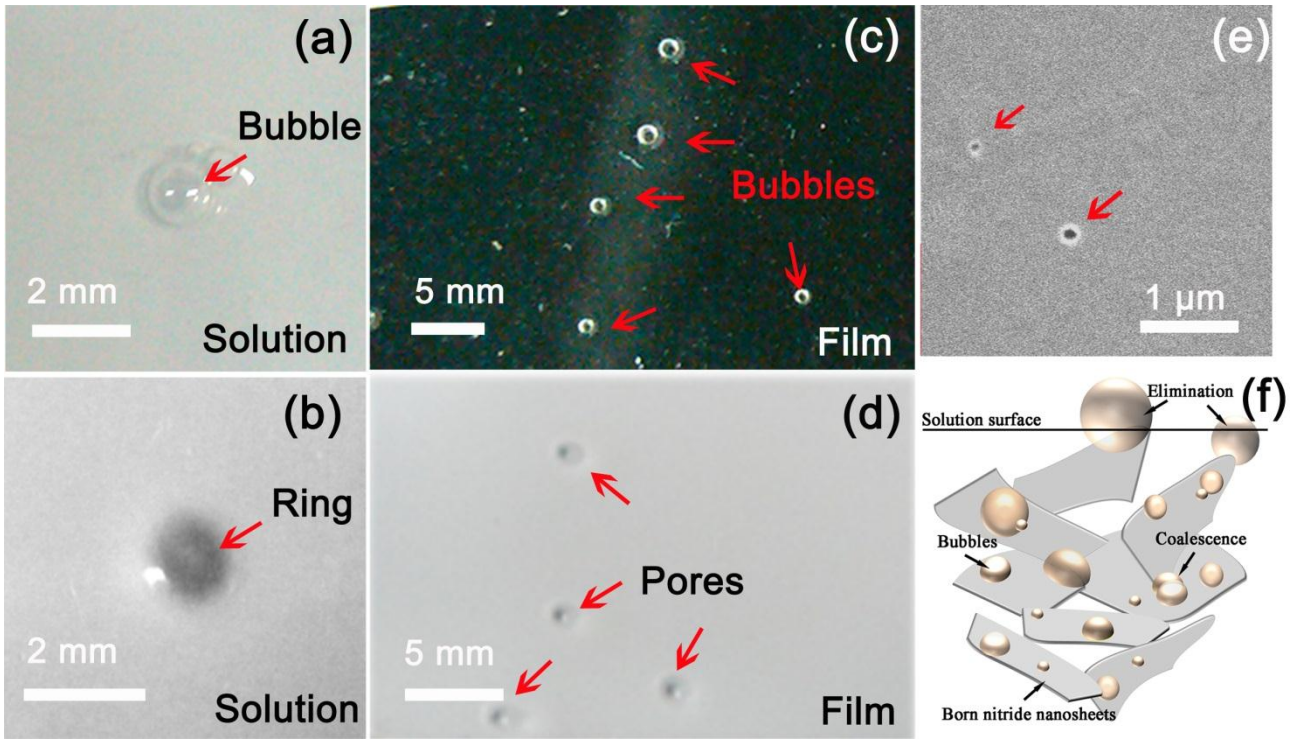

Figure S1. Photographs of bubbles in pure CA solution (a) and film (c) on the black background; White ring in BNNSs/CA solution (b) and residual pores (d) in composite film after bubble elimination; SEM image of small pores in composite film with 1wt% BNNSs loadings(e);The schematic model of the bubbles departure process (f).

Big bubbles (about 1mm in diameter) were generated by injecting a certain amount of air into the solution by the syringe. Different movement behaviors of bubbles occurred in pure CA and BNNSs/CA composite film (Figure S1a, b). Bubbles were easily eliminated from the BNNSs/CA solutions, but pure CA solution showed an opposite tendency. BNNSs could be easily absorbed by bubbles due to high surface energy of BNNSs and minimization surface area of bubbles, and then formed the white ring after bubbles breakup (Figure S1b). Besides, few residual pores were observed in composite film after the elimination of bubbles, further confirming the reducing process of bubbles (Figure S1d, e). By comparison, Figure S1c shows that a few bubbles were hardly eliminated although CA solutions were degassed by prolonging standing time before coating process. Figure S1f shows a schematic model of the process through which small bubbles departed from the composite solution. It is possible to infer the following process: small bubbles captured by BNNSs converge to form a large bubble which was finally eliminated through BNNSs near the surface. Hence, three-dimensional channel formed by BNNSs can increase the degassing speed and provide possibility for enhancing mechanical properties of BNNSs/CA composite.

As has been noted, most bubbles were eliminated through BNNSs, but a few small bubbles might still be deposited by the rapid solidification of CA. However residual bubbles could readily affix themself to the surface of BNNSs. So the stress at the bubble surface could quickly transfer to BNNSs nearby, and then further transfer to CA matrix. On the whole, these transfers might continue until the uniform stress was achieved. Consequently, the addition of BNNSs could increase the degassing speed and reduce the negative effects of bubbles.

TC2: The exfoliated effect of h-BN in acetone containing CA

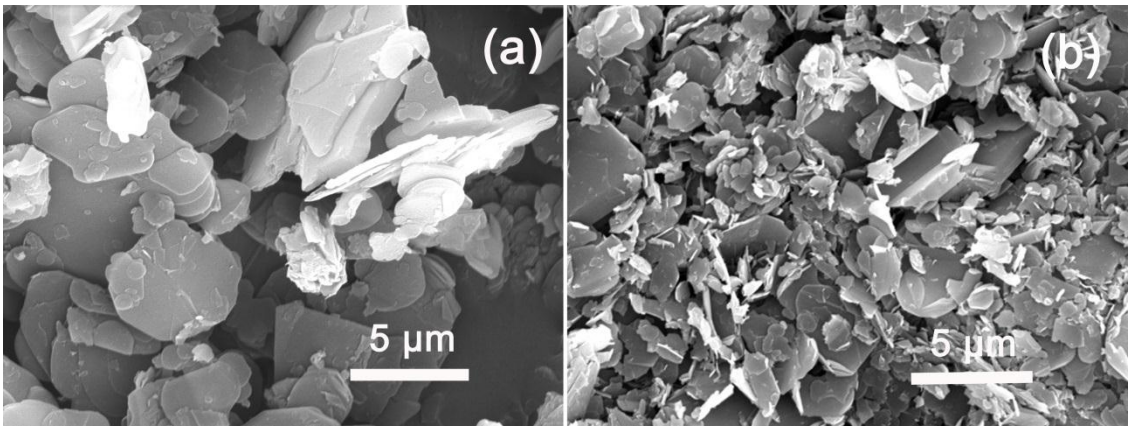

Figure S2. SEM images of h-BN particles before (a) and after (b) exfoliating by sonication.

TC3: The crystallinity properties of h-BN and BNNSs

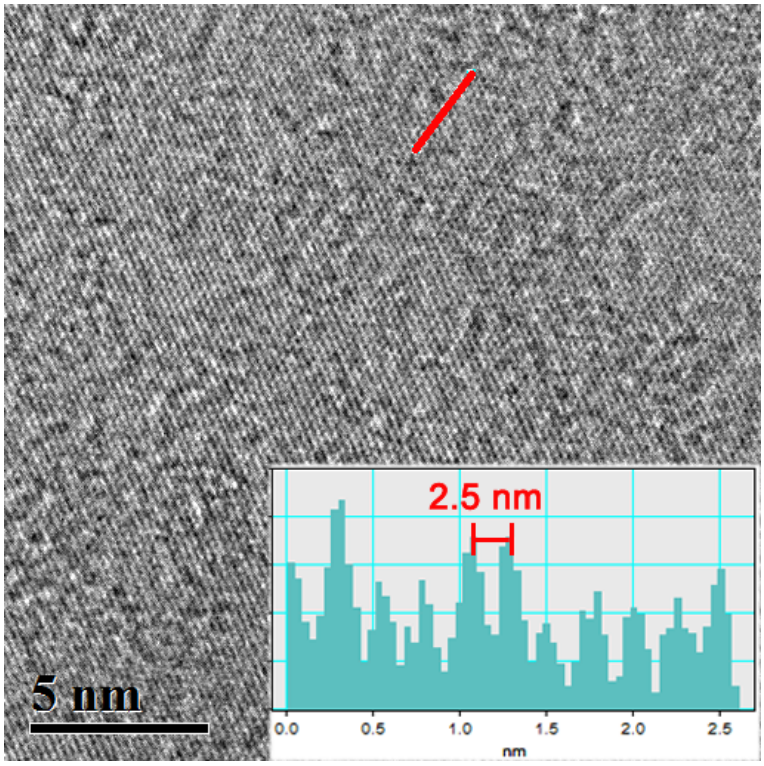

Figure S3. High-resolution TEM images of BNNSs. Inset : the intensity profile recorded along the marked red line shows that the fringe separation is 0.25 nm.

Figure. S3 shows the HRTEM image of BNNSs, and the distance between each two neighboring white dots is actually equal to that of the two nearest N or B atoms. In the inset to Figure S3, the intensity profile reveals that the fringe separation is 0.25 nm. Besides, the layer of h-BN comprised hexagonal arrays of B and N atoms, which indicates high crystalline of BNNSs.

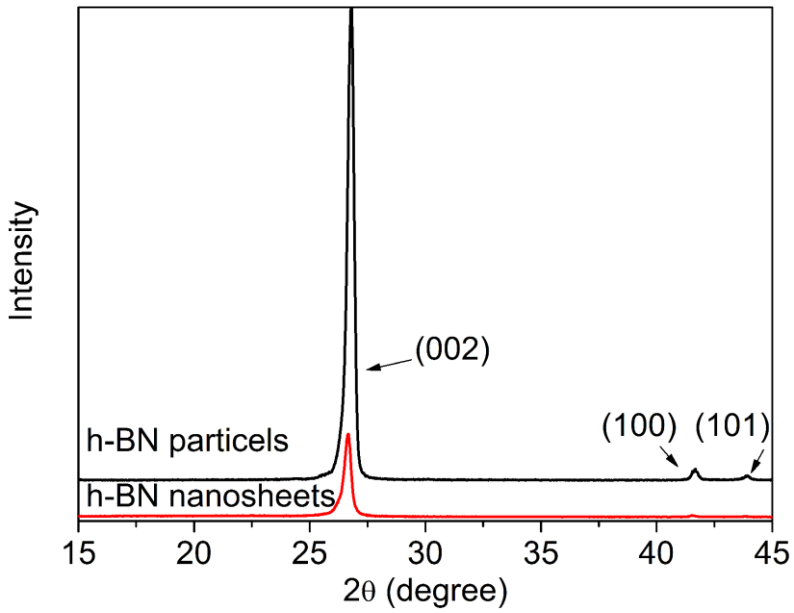

Figure S4. XRD pattern of h-BN and BNNSs

XRD is an important tool for determining crystalline structures and crystallinity. As shown in Figure S4, the hexagonal crystal structure of h-BN and BNNSs was confirmed by X-ray diffraction measurements (XRD). The sharp crystalline peaks indicate that h-BN and BNNSs are highly crystalline. Compared with the pristine h-BN particles, the intensity of the (002) peak of BNNSs obviously decreases, (100) and (101) peaks are hardly observed. These indicate that the sonication did not destroy the short range order of the BN crystals.

TC3: BNNSs for reducing the crack propagation

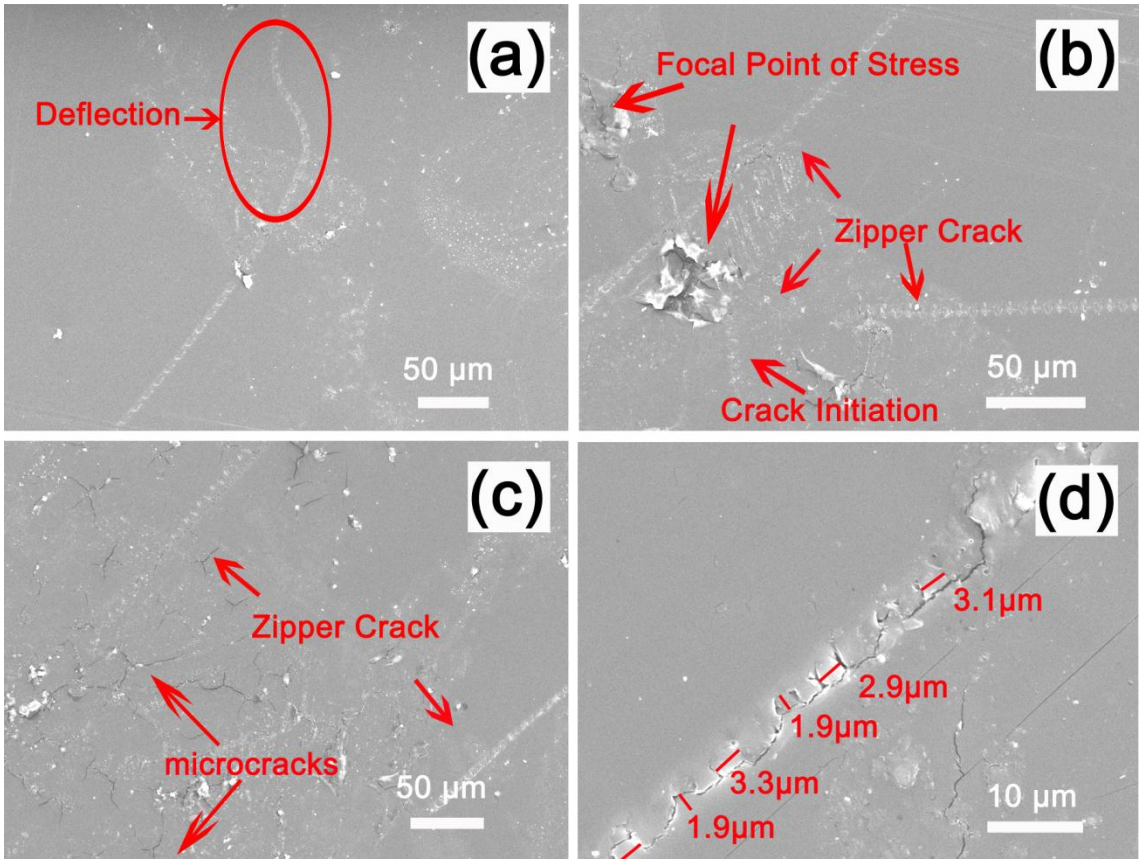

Figure S5. Toughening mechanisms of composites films by embedding BNNSs. SEM images of the deflection (a) and formation region (b, c) of "zipper crack"; High magnification image and red marks show the size of protruding teeth (d); The vertical axis of image is the tensile direction.

Crack is an important means for discussing the toughening mechanism in composites. The filler usually plays a contradictory role in fracture toughness of composites. On one hand the filler can effectively improve the energy barrier for reducing the crack propagation rate. On the other the weak interaction between inorganic phase and organic phase, the aggregation and edges of the fillers can all lead to new stress concentrations. The deflection and slowdown of crack propagation were clearly observed in Figure S5b, c, so the addition of BNNSs is favorable for preventing the continuation of cracks. Obviously, the energy for bypassing the obstacle of large sheets is higher than that of small sheets. In addition, "zipper cracks" were found in composite containing large flakes with relatively uniform size. The starting region of the "zipper cracks" are commonly near the zone of stress concentration, so "zipper cracks" may need enough energy for formation and growth in initial stage. Figure S5a, b also display the deflection and the propagation of "zipper cracks". Above all, the strain direction and "zipper cracks" inclined to one another about an angle of 45 °, reducing the negative effect of the tangential force. This demonstrated that "zipper crack" can significantly improve the energy absorption and reduce negative effects of the stress concentration.

TC4: mechanical properties of composites with different BNNSs contents

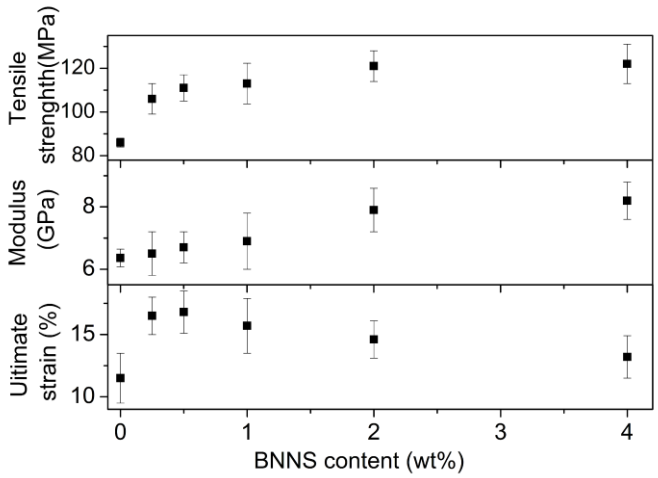

Figure S6. Young's modulus, tensile strength and ultimate strain of pure CA and composite films with different BNNSs loadings. These nanosheets were separated at 1500 rpm

TC5: AO erosion resistance of composites with different BNNSs contents

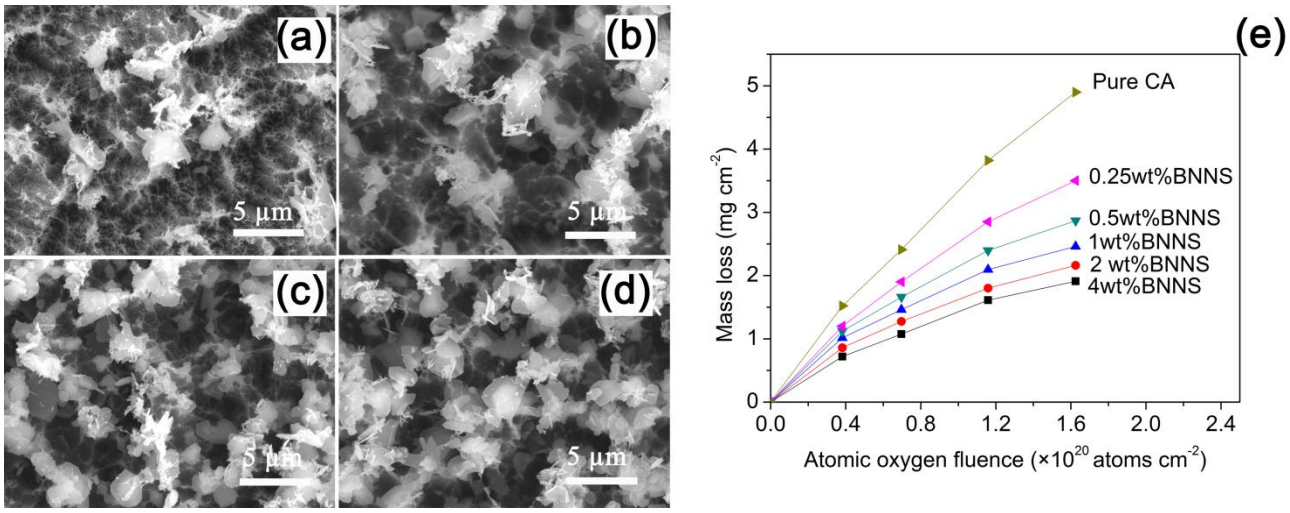

Figure S7. SEM images of composite films with 0.25wt% (a), 0.5wt% (b), 1 wt % (c), 2 wt % (d) BNNSs contents after AO exposure; Mass loss of pure CA and BNNSs/CA composites with various contents after AO exposure (e). These nanosheets were selected with the final rate of 1500 rpm

TC6:TGA results

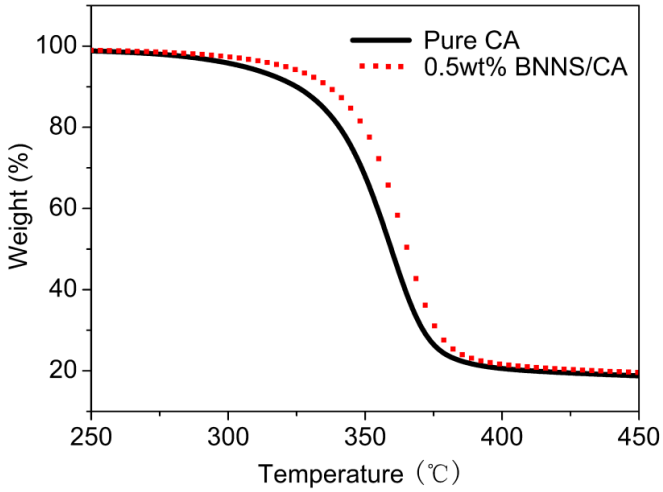

Figure S8. TGA curves of pure CA film and BNNSs/CA composite film containing 0.5 wt% BNNSs content

The thermal properties of pure CA and BNNSs/CA composite film with 0.5 wt% loadings were investigated by thermogravimetric analysis (Figure S8). The temperature of the maximum degradation rate for 0.5 wt% BNNSs/CA composites obtained from the derivative of TGA curves is about 7.5 ℃ higher than that of pure CA. The addition of BNNSs can improve the thermal stability owing to large contact area and strong interface interaction.